Inclusion of the specular component in the assessment of bidirectional distribution functions based on digital imaging

M. Andersen *, J.-L. Scartezzini

Swiss Federal Institute of Technology (EPFL), Solar Energy and Building Physics Laboratory (LESO-PB), Building LE, 1015 Lausanne, Switzerland

Abstract

To describe complex fenestration systems such as novel solar blinds, new glazing or coating materials, daylight and sunlight-redirecting devices, a detailed description of their optical properties is needed, given by their Bidirectional Transmission (or Reflection) Distribution Functions (commonly named BTDFs and BRDFs). These functions are angle-dependent at both the incidence and the emission levels, and are defined as the ratio of the luminance of a surface element in a given direction (after diffuse transmission or reflection) to the illuminance on the sample. However, these functions are capable of describing the specular as well as the diffuse components of emerging light, and their mutual knowledge is necessary to properly assess a glazing or shading system's daylighting performances and benefit from their potential as energy-efficient and users' comfort strategies. Although the analytical expression of a BT(R)DF differs whether it is related to specular or diffuse light, a simultaneous assessment of the two components can be achieved under certain conditions. These conditions are analyzed for the particular data acquisition procedure developed for a novel type of bidirectional goniophotometer, based on digital imaging.

Key words: Bidirectional Transmission (Reflection) Distribution Function (BT(R)DF), Digital imaging (CCD camera), Goniophotometer, Daylighting

1 Introduction

The concept of bidirectional distribution function was first introduced in Nicodemus (1970) and Nicodemus et al. (1977) for directional reflectance in radiometric units, where it was defined as the scattered surface radiance ($W \cdot m^{-2} \cdot sr^{-1}$) divided by the incident surface irradiance ($W \cdot m^{-2}$).

As a photometric quantity (Commission Internationale de l'Eclairage, 1983; Association Française de l'Eclairage, 1991; Schweizerische Lichttechnische Gesellschaft, 1992; Illuminating Engineering Society of North America, 1993), where it is applicable to the detailed characterization of complex fenestration systems, the Bidirectional Transmission (or Reflection) Distribution Function (BTDF or BRDF) and sometimes also named luminance coefficient, q, is defined in Commission Internationale de l'Eclairage (1977) as the "quotient of the luminance of the medium by the illuminance on the medium". It is illustrated in Figure 1 and expressed by Equation (1) in $Cd \cdot m^{-2} \cdot lux^{-1}$ or sr^{-1}:

$$BT(R)DF(\theta_1, \phi_1, \theta_2, \phi_2) = \frac{L_2(\theta_1, \phi_1, \theta_2, \phi_2)}{L_1(\theta_1, \phi_1) \cdot \cos\theta_1 \cdot d\omega_1} = \frac{L_2(\theta_1, \phi_1, \theta_2, \phi_2)}{E_1(\theta_1)} \quad (1)$$

where the corresponding symbols are defined as follows:

* Corresponding author. Present address: Building Technology Program, Department of Architecture, Massachusetts Institute of Technology (MIT), Room 5-418, 77 Massachusetts Avenue, Cambridge MA 02139-4307, USA. Tel: +1-617-253-7714; fax: +1-617-253-6152.

Email address: mand@mit.edu (M. Andersen).

URL: http://architecture.mit.edu/people/profiles/prander.html (M. Andersen).

- (θ_1, ϕ_1) and (θ_2, ϕ_2) are the polar co-ordinates of the incoming and emerging (either transmitted or reflected) light flux, expressed in (°) for convenience [1] ;
- $L_1(\theta_1, \phi_1)$ and $L_2(\theta_1, \phi_1, \theta_2, \phi_2)$ are the luminances of an element of incoming and emerging light flux ($Cd \cdot m^{-2}$);
- $d\omega_1$ is the solid angle subtended by the incoming light flux (sr);
- $E_1(\theta_1)$ is the illuminance on the sample plane due to the incident light flux (lux).

Fig. 1. Photometric and geometric quantities used to define the Bidirectional Reflection (a) and Transmission (b) Distribution Functions of a fenestration material.

As literally expressed by the term "directional", BT(R)DFs are formally defined for differential quantities, i.e. over infinitesimal elements of sample area dA and solid angles $d\omega_1$ and $d\omega_2$. Hence, specular transmittance or reflectance leads to a Dirac function (δ-function) in the direct transmitting (reflecting) direction $(\theta_2, \phi_2) = (\theta_1, \phi_1 + 180°)$.

However, as physical measurements are always made over finite intervals and as the incident beam is never perfectly collimated (for the sun, rays present a 0.25° spread), any measurement becomes an average value over these intervals (Nicodemus et al., 1977; Apian-Bennewitz and von der Hardt, 1998). This also applies to BT(R)DF measurements: the strict directional formalism becomes irrelevant and has to be considered in a broader sense.

As pointed out by Nicodemus et al. (1977), when emerging light distributions vary rapidly, which is typically the case around specular or quasi-specular "peaks", goniophotometric measurement data are very sensitive to the angular-

[1] In this paper, wherever required, angles are explicitly specified in radians.

resolution of the instrument, which makes the figures averaged over the resolution interval of little significance. Integrated or average values for BT(R)DFs over a certain detection area, of appropriate size and configuration, then become more useful than the concept of BT(R)DFs approximating δ-functions.

The bi-conical formalism answers these constraints by resorting to bi-conical distribution functions instead of BT(R)DFs, integrating the latter over the involved incoming and outgoing solid angles ω_1 and ω_2 (Nicodemus et al., 1977; McCluney, 1994). However, this more general formalism is more complex and therefore impractical to handle for daylighting applications. On the other hand, using different formalisms whether the emerging light distribution is diffuse or presents high luminance gradients should be avoided as well. Consequently, a study of the most appropriate detection areas is a resourceful approach in the assessment of bidirectional distribution functions of glazing or shading systems.

This study, outlined in the appendix of Andersen et al. (2003), is presented in this paper, followed by an investigation of how this influences the assessed BT(R)DF data for an innovative bidirectional video-goniophotometer (Andersen, 2004) in the case of complex glazing with strongly specular transmission features such as prismatic panels.

2 BT(R)DF assessment method

The functioning principle of the bidirectional goniophotometer considered in this paper, is extensively described in Andersen (2004) and illustrated by Fig-

ure 2(a). It works in the following manner: light emerging from the sample is reflected by a diffusing triangular panel towards a Charge-Coupled Device (CCD) camera, used as a multiple points luminance-meter and calibrated accordingly (Andersen et al., 2001). The diffusing coating of the screen is necessary both because the camera must be able to capture light reflected by any area of the screen independently of the location of this area and to avoid any correlation between the camera's position and the measurements. The reflection properties of the screen were verified against the lambertian model, and shown to fit the latter closely (discrepancies of only 2.6%, as detailed in Andersen et al. (2001); Andersen (2004)).

After six 60° rotations of the screen-camera system, the emerging light distribution is fully determined in a very short time (a few minutes). For reflection measurements (Figure 2(b)), some additional constraints appear due to the conflict of incident and emerging light flux. The incoming beam needs to penetrate the measurement space and reach exactly the sample surface, therefore requiring a special opening through the measurement space envelope and the removal of screen covers when the latter is obstructive.

Apart from being extremely time-efficient (about three hundred times faster), this assessment method differs from conventional point-per-point investigations of the emerging space with a moving sensor in the way that it splits the emerging hemisphere into a regular grid of averaging zones of freely chosen angular dimensions ($\Delta\theta_2$, $\Delta\phi_2$), which is a way to prevent the user from missing discontinuities in the emerging luminance figure.

Fig. 2. Functioning principle of bidirectional goniophotometer based on digital imaging techniques.

A luminance mapping of the projection screen is carried out by capturing images of it at different integration intervals, thus avoiding over and under-exposure effects, and appropriately combining the latter to extract BT(R)DF data at a pixel level resolution.

At each screen position, a set of images is captured by the CCD camera at all integration times necessary to cover the current luminance dynamic; greyscale levels are then transformed into corresponding luminances and the images appropriately superposed to improve the accuracy of luminance measurements (32 bits values) and avoid over-exposure (saturation) and/or under-exposure in presence of high luminance dynamics. Each pixel's associated screen luminance L_{screen} is then divided by the simultaneously measured illuminance $E_1(\theta_1)$ to achieve a complete $\frac{L_{\text{screen}}}{E_1(\theta_1)}$ mapping of the projection screen.

To obtain a BT(R)DF map, screen reflection, distance and light tilting effects must be compensated, which leads to Equation (2) for the $\frac{L_{\text{screen}}}{E_1(\theta_1)}$ to $BT(R)DF$ conversion (Andersen et al., 2001):

$$BT(R)DF(\theta_1, \phi_1, \theta_2, \phi_2) = \frac{\pi}{\rho_{\text{screen}}} \cdot \frac{d^2(\theta_2, \phi_2)}{A \cdot \cos\alpha \cdot \cos\theta_2} \cdot \frac{L_{\text{screen}}(\theta_1, \phi_1, \theta_2, \phi_2)}{E_1(\theta_1)} \quad (2)$$

where:

- ρ_{screen} is the reflection coefficient of the diffusing screen;
- d is the distance from the sample center to a particular point on the screen along direction (θ_2, ϕ_2);
- A is the sample area (of diameter D);
- α is the angle at which the emerging light reaches the screen.

3 Specular and diffuse components of emerging light flux

From the produced screen luminance maps $L_{\text{screen}}(\theta_1, \phi_1, \theta_2, \phi_2)$, two different types of information can be extracted:

- In the case of scattered light, the $L_{\text{screen}_{\text{diff}}}$ values allow to determine the luminance distribution $L_2(\theta_1, \phi_1, \theta_2, \phi_2)$ emitted by the sample.
- In the case of direct transmittance (resp. reflectance), i.e. specular light flux, $L_{\text{screen}_{\text{spec}}}$ values allow the deduction of the direct transmission (resp. reflection) factor $\tau_{\text{dir}}(\theta_1, \phi_1)$ (resp. $\rho_{\text{dir}}(\theta_1, \phi_1)$), accounting for the source intensity (provided by the simultaneously measured illuminance $E_1(\theta_1)$).

To keep a single conversion for both types of luminances, and assess them using the same method, equivalent expressions must be verified. This will define conditions to be fulfilled when analyzing L_{screen} maps.

Figure 3(a) illustrates the separation of emerging light into diffuse and specular components.

The only distance to be considered in the first case is d, the distance between the detector surface and the sample, as the sample truly becomes a secondary light source; in the second, it is distance $h + d$ from the source to the detection surface that drives the screen illuminance E_{screen} (and thus L_{screen}).

Fig. 3. Specular and diffuse components in the goniophotometric assessment of emerging light.

As a matter of fact, the value to consider for h is not the physical distance from the sample to the source lens or bulb (here equal to 10.3 m). Instead, its virtual distance to an equivalent point source should be considered, as the emitted light beam presents characteristics of a point source emission: the illuminance measured in a plane normal to the incident beam follows Bouguer's law with a correlation of 99%. Therefore, the beam can reasonably be considered as issuing from a point source situated at a distance determined by the rays' spread angle η.

In Andersen (2004), the angular spread, η, of the incident rays reaching the sample area $\pi\frac{D^2}{4}$ was determined experimentally for different sample diameters D by comparing the measured (real source) and theoretically expected (perfectly parallel beam) diameters of illuminated areas on the projection screen in the absence of any sample. η was found to vary between 0.1° and 0.3° with the current light source, and between 0.4° and 1.1° for a previous source, used during an important phase of development of the device and for a substantial set of BTDF measurements (Andersen et al., 2000, 2001) thus also considered in this study, but replaced later by a more powerful and more collimated projector. An average value for the distance h between the virtual point source and the sample, given by $h = \frac{D}{2\tan\eta}$, was thus calculated; it is equal to 25.9 ± 0.3 m for the current light source and to 7.6 ± 0.2 m for the previous one.

The detection principle specific to the present goniophotometer is illustrated in Figure 3(b) for transmission measurements (also valid in reflection mode with the light source on the other side of the sample); S stands for an arbitrary detection area on the projection screen.

To express the screen luminance $L_{\text{screen}_{\text{diff}}}$ due to diffuse emerging light, we can modify Equation (2) into:

$$L_{\text{screen}_{\text{diff}}} = \frac{\rho_{\text{screen}}}{\pi} \cdot \frac{L_2 \cdot A \cdot \cos\theta_2 \cdot \cos\alpha}{d^2} \tag{3}$$

On the other hand, in order to express $L_{\text{screen}_{\text{spec}}}$ due to specularly transmitted or reflected light, we can write $E_{\text{screen}_{\text{spec}}}$ (the illuminance received on the projection screen) in terms of the light source intensity I_1 by Equation (4):

$$E_{\text{screen}_{\text{spec}}} = \tau_{\text{dir}}|\rho_{\text{dir}} \cdot \frac{I_1 \cdot \cos\alpha}{(h+d)^2} \tag{4}$$

where the combined symbol $\tau_{\text{dir}} \,|\, \rho_{\text{dir}}$ is used instead of either τ_{dir} or ρ_{dir} for simplification.

The screen's surface being lambertian, the relation between $E_{\text{screen}_{\text{spec}}}$ and $L_{\text{screen}_{\text{spec}}}$ is given by Equation (5):

$$L_{\text{screen}} = \rho_{\text{screen}} \frac{E_{\text{screen}}}{\pi} \tag{5}$$

As I_1 can be expressed in terms of E_1 using Bouguer's law:

$$I_1 = h^2 \cdot E_1(\theta_1) \tag{6}$$

one obtains Equation (7) for $L_{\text{screen}_{\text{spec}}}$:

$$L_{\text{screen}_{\text{spec}}} = \tau_{\text{dir}}|\rho_{\text{dir}} \cdot \frac{\rho_{\text{screen}}}{\pi} \cdot \frac{h^2 \cdot \cos\alpha}{(h+d)^2} \cdot E_1 \tag{7}$$

4 Conditions for a simultaneous assessment of specular and diffuse light components

Considering Equations (3) and (7) to be equivalent asks relation (8) to be verified:

$$L_2 \approx \tau_{\text{dir}}|\rho_{\text{dir}} \cdot \frac{d^2 \cdot h^2}{(h+d)^2} \frac{1}{A \cdot \cos\theta_2} \cdot E_1 \tag{8}$$

E_1 is defined as the ratio between the incident light flux Φ_1 and the apparent receiving surface $A\cos\theta_1$. As far as L_2 and $\tau_{\text{dir}}\,|\,\rho_{\text{dir}}$ are concerned, they can be expressed in average quantities by Equations (9), where Φ_2 is the emerging light flux and Ω_2 the solid angle around direction (θ_2, ϕ_2):

$$\begin{aligned} L_2 &= \frac{\Phi_2}{A \cdot \cos\theta_2 \cdot \Omega_2} \\ \tau_{\text{dir}}|\rho_{\text{dir}} &= \frac{\Phi_2}{\Phi_1} \end{aligned} \tag{9}$$

We can thus rewrite Equation (8) into (10):

$$\frac{1}{\Omega_2} \approx \frac{d^2 \cdot h^2}{(h+d)^2} \cdot \frac{1}{A \cdot \cos\theta_1} \tag{10}$$

According to the solid angle definition for Ω_2 given by Equation (11):

$$\Omega_2 = \frac{S \cdot \cos\alpha}{d^2} \tag{11}$$

the conditions that have to be fulfilled by the digital imaging-based goniophotometer for assessing both specular and diffuse light components can be expressed by Equation (12):

$$\frac{h^2}{(h+d)^2} \approx \frac{A \cdot \cos\theta_1}{S \cdot \cos\alpha} \tag{12}$$

This conclusion fits very well with intuition: to compensate the fact that the sample is not a point, the detection of the emerging light distribution should be made according to patches that consider luminance peaks as whole entities. Murray-Coleman and Smith (1990) actually made a statement in very good agreement with the above development, by asserting that "when the sample size exactly matches the image of the source in a perfectly specular sample, the correct peak B[T]RDF is measured and spatial resolution is maximized"; it can be noted that this statement assumes the specular component of emerging light flux to be included in a BT(R)DF assessment.

5 Impact on BT(R)DF assessment accuracy

To evaluate how strongly the fulfillment of Equation (12) influences the BT(R)DF data measured with the goniophotometer, a simulation model of the latter was constructed with the commercial ray-tracing software TracePro® [2]. Measured BTDFs for prismatic glazing were compared first to simulated values obtained with a faithful copy of the experimental device, then to simulation results achieved with an ideal set-up model, consisting of optimal components and geometry for a perfect fulfillment of Equation (12) (both simulation models are explained in more detail in Andersen et al. (2003)). This ideal set-up model includes:

- A virtual sun is chosen as the light source, presenting a beam spectrum as close as possible to the real sun and showing perfectly parallel rays.
- The detection surface is hemispherical and perfectly absorbing to avoid inter-reflections; in addition to this, an optimized diameter is determined

[2] TracePro® Expert - 2.3 & 2.4.0 releases, Lambda Research Corp.

for the detector to satisfy Equation (12): as the light source is considered infinitely far away, the ratio $\frac{h^2}{(h+d)^2}$ tends towards 1, and therefore, the ratio $\frac{A \cdot \cos\theta_1}{S \cdot \cos\alpha}$ (with $\cos\alpha = 1$ as the averaging areas S are normal to the rays for a hemispherical detector) has to come as close to 1 as possible.

The experimental conditions impose given values on both the sample area A and the averaging grid resolution ($\Delta\theta_2$, $\Delta\phi_2$); hence, the values of S over the hemisphere will be determined only by the virtual detector's radius. The latter is therefore calculated in order that the average value of the right-hand part of Equation (12) equals 1 over the default set of 145 incident directions (θ_1, ϕ_1).

By observing the discrepancies between BTDF data obtained for optimal conditions (ideal model) and measurements or simulated values for a model faithful to the experimental conditions, one can find out how the fulfillment of Equation (12) influences the accuracy of the results, and to what extent an approximation is acceptable. Figure 4 provides the comparative results obtained for different incident directions and prism gratings geometries.

Fig. 4. Relative difference between experimental conditions (measurements or simulations) and ideal set-up model due to the approximate fulfillment of Equation (12). The relative discrepancies are defined for various incident directions and emerging angles (θ_2, ϕ_2).

As h is equal to 25.9 m (resp. 7.6 m with the previous source) and as the average distance d from the sample to the diffusing screen is 0.905 m, the mean distance ratio is equal to 0.93 (resp. 0.80), whereas the average value of the area ratio is 1.01 for the default diameter $D = 10$ cm and averaging grid intervals ($\Delta\theta_2$, $\Delta\phi_2$) = (5°, 5°). Besides, as the screen is a flat surface, d is

a function of θ_2 and ϕ_2, inducing that the fulfillment of Equation (12) will, at best, only be possible on an average and not for all individual directions (θ_2, ϕ_2).

Fortunately, the experimental conditions, that only verify Equation (12) within a 10% margin (resp. 22% for the previous source), induce lower relative impact on achieved BTDF values: amongst the discrepancies observed on Figure 4 for the two sources, more than 9 out of 10 are inferior to 7% (to 10% for the previous source).

This shows that although Equation (12) is only approximately fulfilled for the present goniophotometer set-up, BTDF results (and likewise BRDFs) remain coherent and reliable even for the specular light distributions of prismatic panels. On one hand, this statement supports the assumptions made for the building up of the device; on the other hand, it makes the simultaneous measurement of diffuse and specular components of light acceptable and suggests to revisit in the future the formal CIE definition for BT(R)DFs (Commission Internationale de l'Eclairage, 1977).

Of course, this assessment method leads to BT(R)DF average values not only related to the emerging rays direction, but also to the angular areas where these rays are detected. This has however no significant effect on the monitored data as long as the sample to detector distance is large compared to the sample size, a factor of 10 being accepted as reasonable. This restriction is verified satisfactorily for the most usual sample diameters ($D \leq 15$ cm); as larger D values are chosen only with coarse averaging grid intervals, it becomes less critical to avoid a small correlation with the distance parameter.

6 Conclusion

Bidirectional distribution functions are formally only applicable in reference to scattered radiation and would in consequence have to be assessed separately from the possible specular component of transmitted (reflected) light flux (Commission Internationale de l'Eclairage, 1977). This restriction makes it quite laborious to characterize a system properly, as two full investigations are hence required; furthermore, the distinction between highly directional scattering and true specular peaks becomes difficult to establish when dealing with real - thus imperfect - experimental conditions: the incident beam is not perfectly collimated, which induces that even specular transmittance or reflectance will have a non-zero spread.

However, when the BT(R)DF assessment method relies on the splitting of the emerging hemisphere into a grid of adjacent angular zones inside which BT(R)DF values are averaged, the simultaneous assessment of both components can be accepted under specific geometric conditions, that are presented in this paper. They determine a compromise to find between the distances from the sample to the source or the detector, and the apparent areas of the sample and the averaging zones.

In order to estimate how strongly these geometric conditions influence the accuracy of BT(R)DF results achieved with a digital imaging-based photogoniometer, two ray-tracing simulation models of the latter were constructed: one as faithful as possible and the other based on optimal components and geometry that fulfilled the conditions perfectly. The comparison of BT(R)DF results showed that the assumptions made in the design of the instrument

were reasonable, the assessment method allowing as a consequence to measure diffuse and specular components together, which suggests to revisit in the future the formal CIE definition of the corresponding photometric figure.

Acknowledgements

Marilyne Andersen was supported by the Swiss National Science Foundation, fellowship 81EL-66225, during her stay at the Lawrence Berkeley National Laboratory. The authors wish to thank Dr. Michael Rubin and Dr. Joseph Klems at LBNL, as well as Dr. Ross McCluney at the Florida Solar Energy Center for their kind help and advice in BT(R)DF formulation. They would also like to acknowledge Lambda Research Corporation for having provided them with a license of TracePro® to perform simulation model comparisons.

References

Andersen, M., 2004. Innovative bidirectional video-goniophotometer for advanced fenestration systems. Ph.D. thesis, EPFL, Lausanne.

Andersen, M., Michel, L., Roecker, C., Scartezzini, J.-L., May 2001. Experimental assessment of bi-directional transmission distribution functions using digital imaging techniques. Energy and Buildings 33 (5), 417–431.

Andersen, M., Rubin, M., Scartezzini, J.-L., February 2003. Comparison between ray-tracing simulations and bi-directional transmission measurements on prismatic glazing. Solar Energy 74 (2), 157–173.

Andersen, M., Scartezzini, J.-L., Roecker, C., Michel, L., May 2000. Bi-

directional Photogoniometer for the Assessment of the Luminous Properties of Fenestration Systems. CTI Project 3661.2, LESO-PB/EPFL, Lausanne.

Apian-Bennewitz, P., von der Hardt, J., August 1998. Enhancing and calibrating a goniophotometer. Solar Energy Materials and Solar Cells 54 (1-4), 309–322.

Association Française de l'Eclairage, 1991. La photométrie en éclairage. Société d'Editions Lux, Paris.

Commission Internationale de l'Eclairage, 1977. Radiometric and photometric characteristics of materials and their measurement. CIE 38 (TC-2.3).

Commission Internationale de l'Eclairage, 1983. The basis of physical photometry. CIE 18.2 (TC-1.2).

Illuminating Engineering Society of North America, 1993. Lighting Handbook. IESNA, New York.

McCluney, R., December 1994. Introduction to Radiometry and Photometry. Artech House, Boston.

Murray-Coleman, J., Smith, A., 1990. The Automated Measurement of BRDFs and their Application to Luminaire Modeling. Journal of the Illuminating Engineering Society 19 (1), 87–99.

Nicodemus, F., June 1970. Reflectance nomenclature and directional reflectance and emissivity. Applied Optics 9 (6), 1474–1475.

Nicodemus, F., Richmond, J., Hsia, J., Ginsberg, I., Limperis, T., October 1977. Geometrical Considerations and Nomenclature for Reflectance. Nbs monograph 160, National Bureau of Standards, U.S. Department of Commerce, Washington, DC.

Schweizerische Lichttechnische Gesellschaft, 1992. Handbuch für Beleuchtung. Ecomed Verlag, Landsberg.

List of Figures

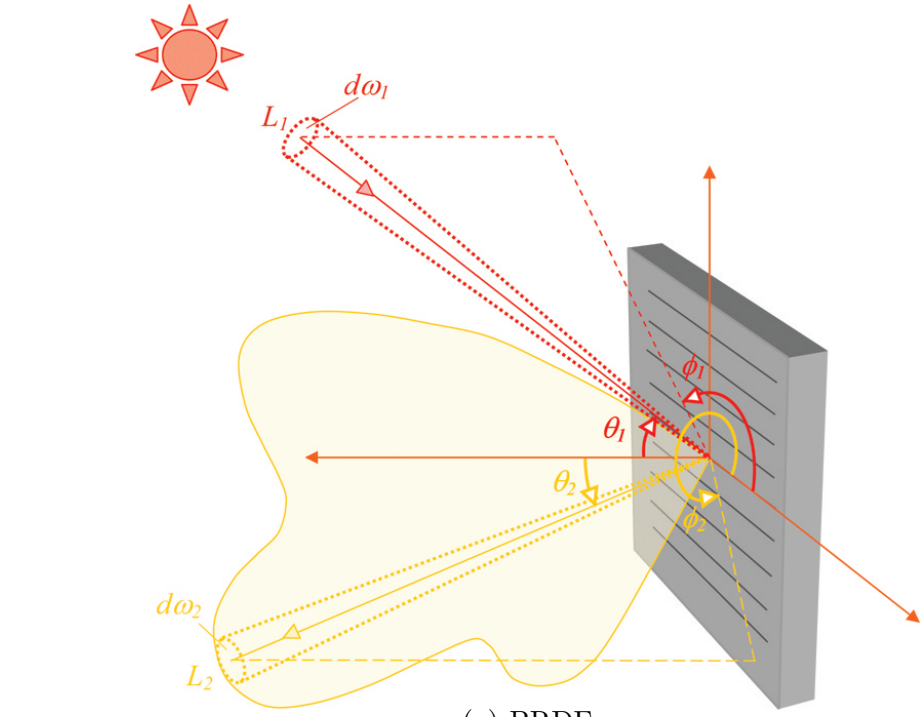

(a) BRDF

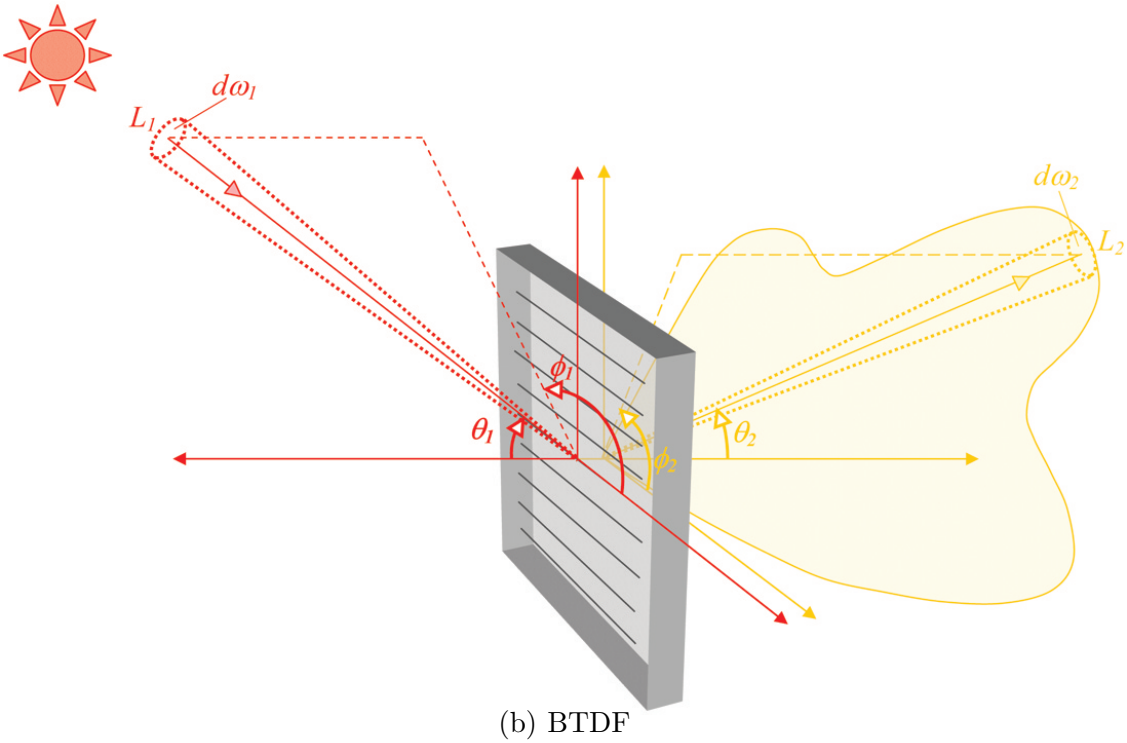

(b) BTDF

Fig. 1. Photometric and geometric quantities used to define the Bidirectional Reflection (a) and Transmission (b) Distribution Functions of a fenestration material.

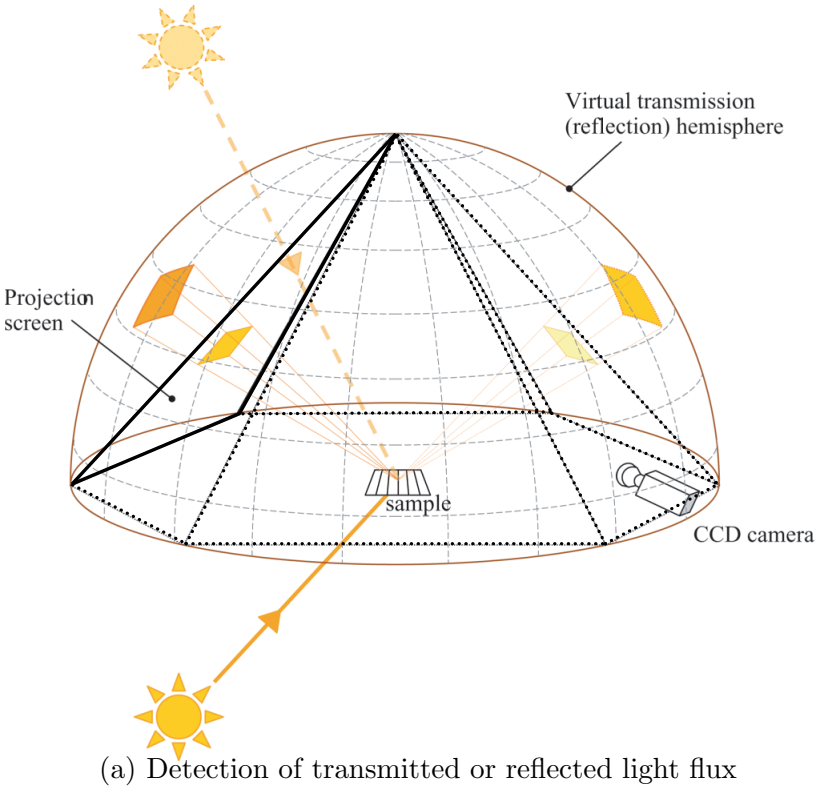

(a) Detection of transmitted or reflected light flux

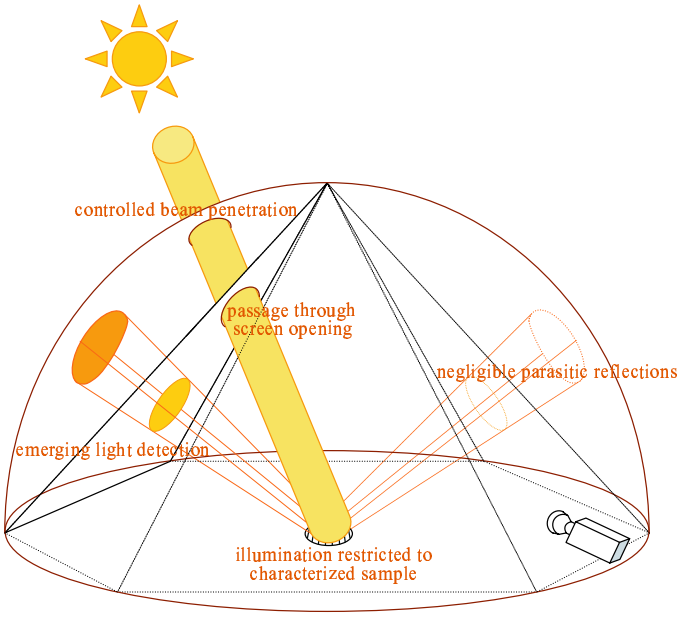

(b) Additional constraints for reflection measurements

Fig. 2. Functioning principle of the bidirectional goniophotometer using a CCD camera pointed towards a flat and diffusing projection screen.

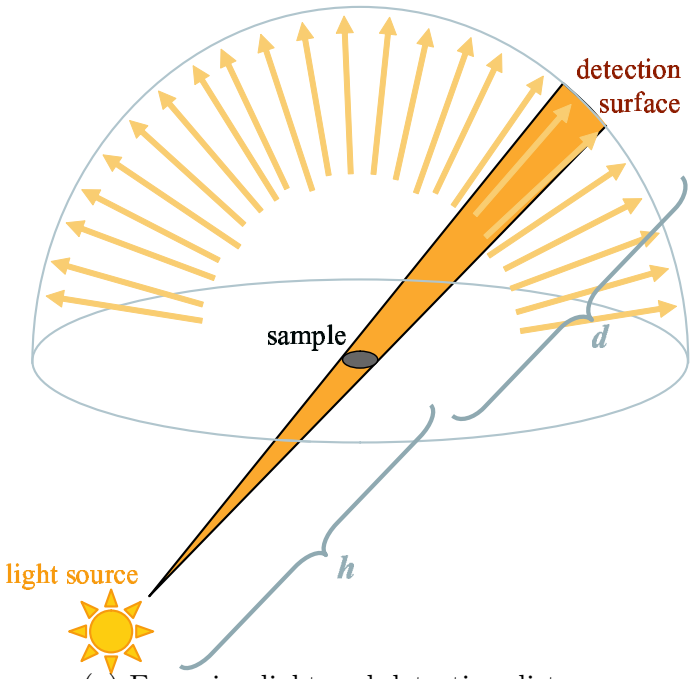

(a) Emerging light and detection distance

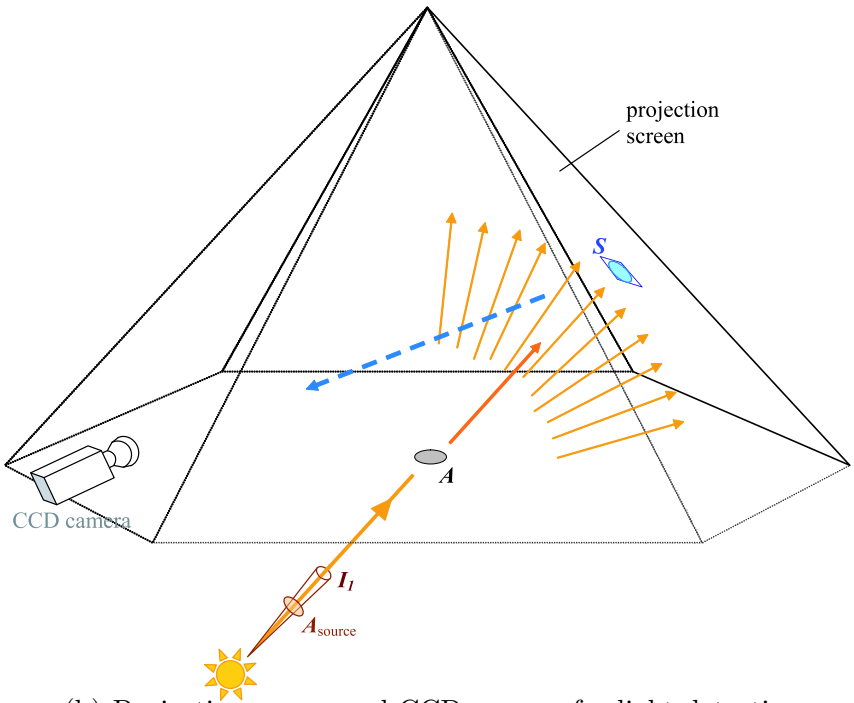

(b) Projection screen and CCD camera for light detection

Fig. 3. Specular and diffuse components in the goniophotometric assessment of emerging light.

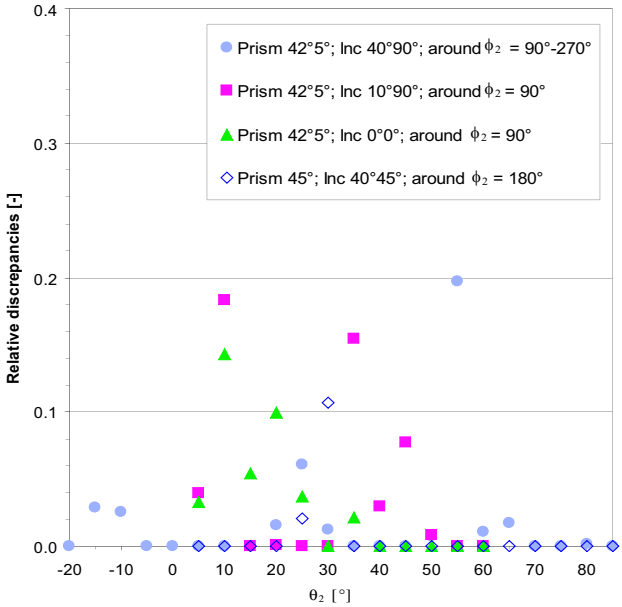

(a) Previous light source

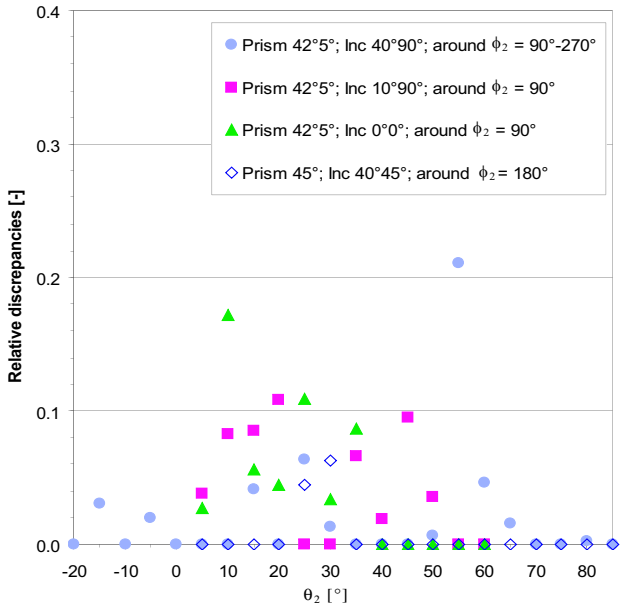

(b) Current light source

Fig. 4. Relative difference between experimental conditions (measurements or simulations) and ideal set-up model due to the approximate fulfillment of Equation (12). The relative discrepancies are defined for various incident directions and emerging angles (θ_2, ϕ_2).